

Hydration of cordierite and hypersthene and a description of the retrograde orthoamphibole isograd in the Limpopo belt, South Africa

DIRK D. VAN REENEN

Department of Geology, Rand Afrikaans University, Johannesburg 2000, South Africa

ABSTRACT

The transition from orthopyroxene- to orthoamphibole-bearing assemblages in Mg-rich metapelites across a retrograde M3 orthoamphibole isograd in the Archean Limpopo belt in South Africa is expressed by two hydration reactions that are superposed on M2 corona textures of cordierite and hypersthene after garnet: hypersthene + quartz + H₂O = anthophyllite, and cordierite + H₂O = gedrite + kyanite + quartz. The temperature of hydration at the isograd of less than 625–650°C at a minimum pressure of 6 kbar is estimated on the basis of (1) a comparison of published information on the solvus in the orthoamphibole system to the results of the present study, (2) the presence of kyanite coexisting with anthophyllite and gedrite both at and south of the isograd, and (3) the application of the garnet-biotite thermometer. The estimated temperature is far below the upper thermal stability limit of anthophyllite under conditions where $P_{\text{H}_2\text{O}} = P_{\text{total}}$.

Cordierite at the isograd is partly (or completely) surrounded by gedrite and kyanite, and hypersthene by anthophyllite; coexisting hypersthene + anthophyllite + quartz is restricted to a narrow zone defined by the isograd. A modified Redlich-Kwong equation of state for nonideal mixing of H₂O and CO₂ was used to calculate the mole fraction of CO₂ (about 0.8) in the fluid phase necessary to displace the equilibrium curve anthophyllite = 7 enstatite + quartz + water to the estimated *P-T* conditions on the isograd. The presence of a systematic temperature gradient in the Limpopo belt suggests that the influx of the CO₂-rich fluid occurred at a fixed temperature during hydration.

INTRODUCTION

The Archean high-grade Limpopo belt of southern Africa is a polymetamorphic, highly deformed terrane situated between the Rhodesian and Kaapvaal cratons (Fig. 1). It has been subdivided into northern and southern marginal zones, which are separated from a central zone by major east-northeast-trending parallel ductile shear zones, the Palala shear zone in the south and the Tuli-Sabi cataclastic zone in the north (Mason, 1973; Robertson and Du Toit, 1981).

The southern marginal zone consists almost entirely of two major categories of rocks that represent metamorphosed and structurally transformed granite- and greenstone-type material of the adjoining Kaapvaal craton (Mason, 1973; Robertson and Du Toit, 1981; Du Toit and van Reenen, 1977; Du Toit et al., 1983; van Reenen, 1983a), including gray migmatized tonalitic and trondhjemitic gneisses (the Baviaanskloof Gneiss) and pelitic, mafic, and ultramafic supracrustals of the Bandelierkop Formation that occur as a series of easily recognizable discontinuous keels surrounded by the Baviaanskloof Gneiss (Fig. 2). The Matok charnockitic-granitic pluton and the Schiel alkaline pluton that straddle a retrograde orthoamphibole isograd (Fig. 2) intruded the metamorphic rocks at 2620 Ma (Barton et al., 1983). The high-grade rocks were affected by three early folding events,

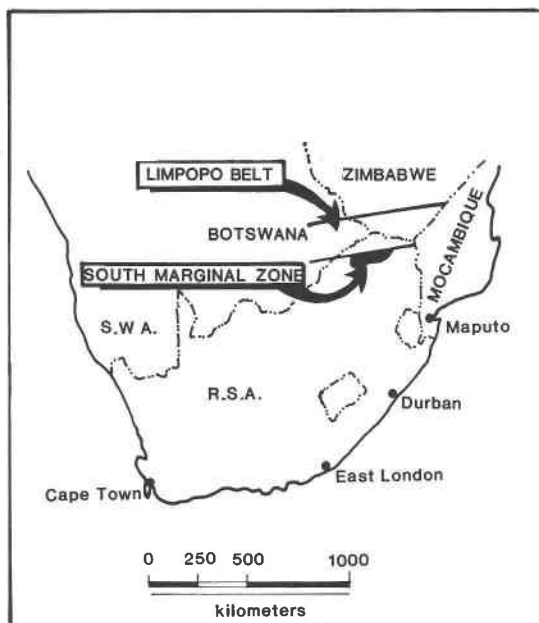


Fig. 1. Sketch map showing position of southern marginal zone of Limpopo belt in South Africa.

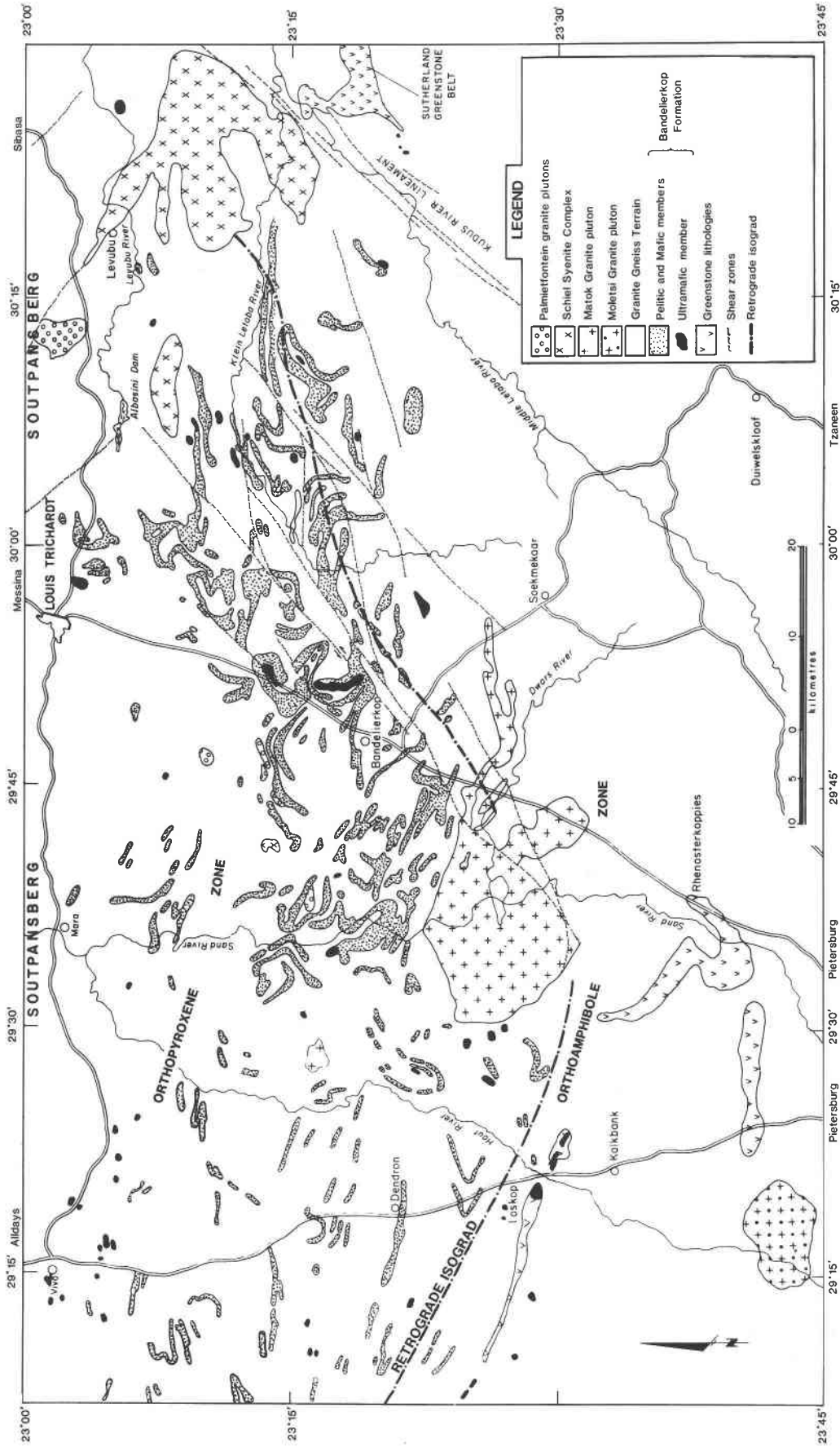


Fig. 2. Geologic map of southern marginal zone of Limpopo belt, showing distribution of metamorphic zones (after Du Toit et al., 1983, and van Reenen, 1983a).

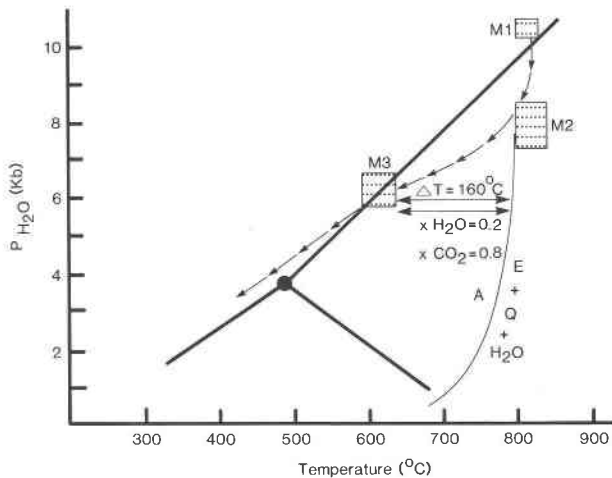


Fig. 3. P - T diagram illustrating uplift and erosion path for southern marginal zone of Limpopo belt. Boxes represent estimated P - T conditions for M1, M2, and M3. Also shown are (1) the calculated (endmember) dehydration curve for the reaction anthophyllite = 7 enstatite + quartz + water under conditions where $P_{\text{H}_2\text{O}} = P_{\text{total}}$ and (2) amount of lowering of $f_{\text{H}_2\text{O}}$ needed to displace this curve to the M3 P - T estimates. See text for discussion.

and a later deformational event is recognized by post-metamorphic shear zones that cut across earlier structures; along the shear zones the high-grade rocks have been retrograded to greenschist-facies assemblages (Du Toit et al., 1983).

The goals of this contribution are to (1) describe an isograd established by retrogression of orthopyroxene-bearing, MgO-rich, metapelitic gneisses of the Bandelierkop Formation in the southern marginal zone into orthoamphibole-bearing gneisses and (2) estimate P - T conditions for the retrograde reactions and thereby calculate the fluid composition associated with retrogression.

METAMORPHIC EVOLUTION OF THE SOUTHERN MARGINAL ZONE

The retrograde orthoamphibole isograd is a conspicuous regional metamorphic feature of this area. This isograd cuts across the structural trend of all lithologic units and can be followed for a distance of at least 150 km from west to east (Fig. 2). It separates an orthoamphibole zone in the south from an orthopyroxene zone in the north and can be limited to a distance of not more than a few hundred meters at right angles to its regional trend. The systematic regional distribution of the metamorphic zones and the position of the isograd in Figure 2 are controlled by a retrograde event (M3) that followed on two earlier granulite events (M1 and M2) before 2500 Ma (van Reenen, 1981, 1983a; van Reenen and Du Toit, 1977, 1978; Du Toit et al., 1983).

Peak metamorphic conditions of $T > 820^\circ\text{C}$ and $P > 9.5$ kbar were attained during the early prograde stage (M1, Fig. 3) of this extended period of high-grade meta-

morphism; this was followed by rapid uplift (M2, Fig. 3), which is recorded by corona textures of cordierite and hypersthene after garnet (Fig. 4a). P - T conditions of this M2 event are $\sim 800^\circ\text{C}$ and 8.6–7.2 kbar (van Reenen, 1983a). The retrograde reactions (M3, Fig. 3) discussed in the present paper were superimposed on the M2 assemblages.

DESCRIPTION OF THE RETROGRADE ISOGRAD

The retrograde isograd, which is only defined within the pelitic gneisses, is discussed in terms of changes, across the isograd, in (1) mineral assemblages observed in metapelitic gneisses, (2) the chemistry of minerals such as garnet and biotite; and (3) hydration reactions that are texturally preserved in metapelitic gneisses.

Changes in mineral assemblages across the isograd

The orthopyroxene zone, situated to the north of the isograd, is characterized by the ubiquitous presence of orthopyroxene in all suitable rock types, including banded iron formation, ultramafic, mafic, and pelitic granulites, as well as some members of the Baviaanskloof gneiss. The mineralogy of representative samples of the metapelitic gneisses in the three metamorphic zones is shown in Table 1. Hydrous phases, such as biotite in the metapelites and hornblende in the mafic and ultramafic granulites, are present in small amounts. Rocks containing exclusively hydrous minerals are entirely restricted to narrow shear zones that crosscut all previous structures.

The pelitic gneisses in the orthopyroxene zone are characterized by three main petrographic types based on the presence or absence of cordierite and/or garnet (Table 1). These assemblages have been the subject of an investigation (van Reenen, 1983a) of the phase relations involving coexisting cordierite + garnet + hypersthene + biotite in order to determine the distribution of pressure and temperature within the orthopyroxene zone during the first (M2) retrograde granulite event. It was shown (van Reenen, 1983a) that the phase relations involving these minerals were controlled by a continuous Fe-Mg reaction (garnet + quartz = cordierite + hypersthene; Figs. 4a, 11a), the nature of which in turn was controlled by subtle differences in bulk chemistry (van Reenen, 1983a, p. 152) during a period of nearly isothermal uplift from granulite facies conditions.

Compositionally similar rocks in the orthoamphibole zone are characterized by the presence of coexisting anthophyllite + gedrite + kyanite in rocks of suitable bulk composition (Table 1) and by the presence of cordierite only as a rare reactant. The position of the retrograde isograd is defined by coexisting anthophyllite and hypersthene in more Fe-rich rocks, or by the presence of hypersthene, anthophyllite, cordierite, and gedrite in more Mg-rich rocks (Table 1).

Modal compositions of representative samples of the pelitic gneisses from the orthoamphibole zone are listed in Table 2. The orthoamphibole-bearing rocks in this table (and in Table 1) are subdivided into a number of different

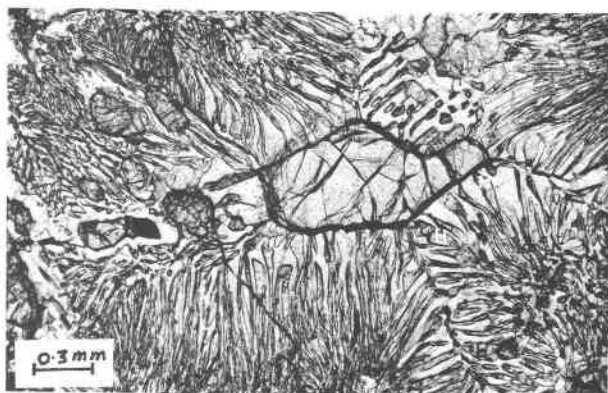


Fig. 4a. The continuous Fe-Mg reaction garnet (Ga) + quartz = cordierite (C) + hypersthene (H) in the cordierite-garnet granulites (Group 2P, Table 1) in the orthopyroxene zone formed by the M2 event (sample DV56).



Fig. 4b. Kyanite (K) intergrown with biotite and orthoamphibole (O) (sample DV43).

mineralogical types based on subtle differences in both mineralogy and bulk chemistry. None of these rocks contain K-feldspar and all contain quartz. Kyanite is usually, but not always, present in small amounts (Table 2) in the orthoamphibole-bearing samples of Groups 1A and 2A as short stubby crystals intimately associated with orthoamphibole (Fig. 4b). It is generally an inconspicuous mineral except in one sample (M215) where it occurs as well-defined prismatic grains scattered throughout the rock (Fig. 4c). Coexisting orthoamphiboles are discussed below. The retrograde M3 activity, based on the persistence of reactant cordierite, extended at least 5 km to the south of the retrograde isograd in Figure 2.

Changes in mineral chemistry across the isograd

The change in the metamorphic conditions across the isograd is not only reflected in the mineralogy of the pelitic gneisses but also by systematic changes in the chemistry of garnet and biotite (Fig. 5) that correspond with the position of the isograd based on textural evidence. The observed increase in the pyrope content of garnet and the Ti content of biotite in going from the orthoamphibole zone through the isograd to the orthopyroxene zone was observed in chemically similar rocks, and this change is so systematic that the position of the isograd can be mapped on the basis of the composition of these two minerals.

Hydration of cordierite and hypersthene along the isograd

The position of the retrograde isograd in Figure 2 is also defined by hydration reactions involving both cordierite and hypersthene. Most hypersthene grains in both the cordierite-bearing (DV3, DR157, M346 of Group 2I in Table 1) and cordierite-free rocks (DV38 of Group 3I in Table 1) are partly (Fig. 6a) or completely replaced by anthophyllite, and this hydration reaction is restricted to the retrograde isograd. Coexisting hypersthene, anthophyllite, and quartz are consequently also restricted to a narrow zone defined by this isograd.

Cordierite along the isograd is always intergrown with a relatively coarse grained aggregate of gedrite (and sometimes also of anthophyllite) and kyanite (Fig. 6b). The aggregate generally appears to have nucleated at cordierite-cordierite grain boundaries and to have grown into the cordierite. This is illustrated in Figure 6c, which shows the incipient hydration of cordierite in the orthopyroxene zone. The process is identical, but the products are much finer grained than those observed along the isograd. Vernon (1972) described similar hydration processes from the Arunta Complex in central Australia. Two generalized reactions are relevant: hypersthene + quartz + H₂O = anthophyllite and cordierite + H₂O = gedrite + kyanite + quartz.

PETROCHEMISTRY

Bulk chemical analyses were done by the General Superintendent Company, Johannesburg, using standard gravimetric, volumetric, and X-ray fluorescence methods. The chemical compositions of 8 representative samples of the pelitic gneisses in Table 1 are given in Table 3. Microprobe analyses were obtained with a nine-spectrometer automated ARL model SEMQ electron microprobe at the Anglo American Research Laboratories in Johannesburg.



Fig. 4c. Coarse-grained kyanite coexisting with orthoamphibole (O) (sample M215).

Table 1. Mineralogical and chemical subdivision of pelitic gneisses from each metamorphic zone

Metamorphic Zone	Mineral Assemblages	MgO/(MgO + FeO)	Discussion
(P) Orthopyroxene Zone	<p>1. C + H + B + Pl(An 28.5) + Q + Sp + K + Ore</p> <p>2. C + H + Ga + B + Pl(An 28.5) + Q + Sp + K + ore</p> <p>3. Ga + H + B + Pl(An 33.4) + Q + ore</p>	<p>0.7 to 0.76 (Group 1P)</p> <p>0.6 to 0.7 (Group 2P)</p> <p>0.53 to 0.59 (Group 3P)</p>	<p>Ga reacted completely in these Mg-rich rocks due to the divariant reaction (below) during M₂.</p> <p>Coexistence of C + Ga + H during M₂ is controlled by the divariant reaction (Fig. 3a): Ga + Q = C + H.</p> <p>Ga in these Fe-rich rocks shows no sign of the divariant reaction.</p>
(A) Orthoamphibole Zone	<p>1. A + G + B + K + Pl(An 34) + Q + ore (DV1)</p> <p>2. (i) A + G + Bi + K + Ga + Pl (An 30) + Q + ore (DV43, DV22)</p> <p>(ii) G + Bi + Ga + Pl(An 30) + Q + ore (M447)</p> <p>3. A + Ga + B + Pl + Q + ore</p> <p>4. G + Ga + Q + ore (DR184)</p>	<p>0.74 (Group 1A)</p> <p>0.6 to 0.65 (Group 2A)</p> <p>0.6 to 0.67 (Group 2A)</p> <p>0.53 to 0.59 (Group 3A)</p> <p>0.50</p>	<p>Absence of Ga due to divariant reaction during M₂.</p> <p>Presence of coexisting orthoamphiboles and K due to hydration of C and H along the isograd (M₃).</p> <p>Presence of coexisting A + G + K controlled by the hydration of cordierite and hypersthene along the isograd during M₂. Presence of Ga controlled by MgO/(MgO + FeO)-ratio of rock (compare Group 2P).</p> <p>Absence of G (and K) due to absence of cordierite in Group 3P in the orthopyroxene zone.</p>
(I) Isograd (Retrograde)	<p>1. C + H + A + G + K + B + Pl + Q + ore (M346)</p> <p>2. C + H + A + G + K + B + Ga + Pl (An 31) + Q + ore (DR157 and DV3)</p> <p>(i) K - G - Q + C</p> <p>(ii) K - Q - G - A</p> <p>(iii) H - Q - A + G</p> <p>(iv) C - G - K - Q</p> <p>3. H + A + Ga + B + Pl(An 31) + Q + ore (DV38)</p>	<p>0.7 to 0.76 (Group 1I)</p> <p>0.6 to 0.7 (Group 2I)</p>	<p>Absence of Ga due to completion of divariant reaction (Compare Group 1P).</p> <p>1 and 2 refer to apparent assemblages. The actual coexisting sub-assemblages in sample M346 are listed under (i) to (iv). Each individual assemblage is arranged in relative order of abundance of the minerals.</p> <p>Absence of C (G and K) controlled by MgO/(MgO + FeO)-ratio of rock. Compare Group 3P.</p>

*Chemical similar rocks from the three zones (P, I and A) are grouped together (e.g. Groups 1P, 1A and 1I). 1, 2 and 3 in each zone designates high, medium and low Mg/Fe respectively. Numbers in parenthesis (e.g. DV1) refer to samples for which chemical data are provided (Tables 3, 4a, 4b and 4c). Abbreviations: A = antophyllite; B = biotite; C = cordierite; G = gedrite; Ga = garnet; H = hypersthene; K = kyanite; Kf = K-feldspar; ore = magnetite, ilmenite, graphite, pyrrhotite, chalcopyrite, pyrite; Pl = plagioclase; Q = quartz; Sp = spinel.

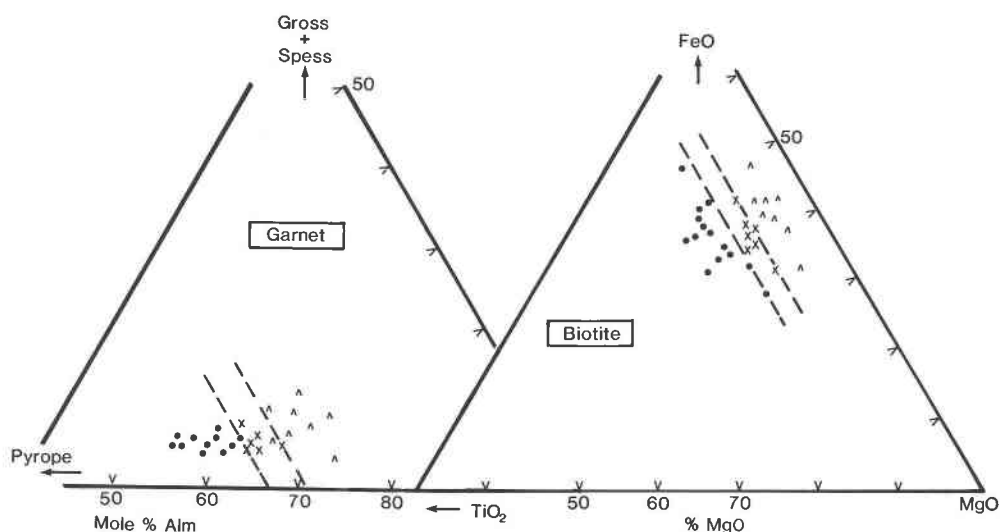


Fig. 5. Variation in composition of garnet and biotite in pelitic gneisses across isograd; ● = orthopyroxene zone, × = isograd, △ = orthoamphibole zone.

Mineral chemistry

Microprobe analyses of cordierite, hypersthene, garnet, biotite, anthophyllite, and gedrite from seven representative samples of the different mineralogical groups (Table 1) are listed in Tables 4 to 8. The results in these tables are mean values for at least two spot analyses of the same grain of the same mineral in the same thin section. A systematic check for evidence of chemical zonation was made only in the case of garnet, where care was taken to obtain point analyses from both the core and the rim composition of each analyzed grain.

Garnets (Table 4) show evidence of chemical zonation, but no detailed zoning profiles were obtained. The general zoning patterns appear rather irregular, and this is quite different from the situation in the orthopyroxene zone where regular zoning patterns (pyrope-rich cores and almandine-rich rims) could be ascribed to the resorption of garnet during the reaction garnet + quartz = cordierite + hypersthene (van Reenen, 1983a). The combined grossular and spessartine content ranges from 4.8 to 12.8 mol% with a mean value of 7.6 mol%.

The mean octahedral site occupancy for all the analyzed biotites (Table 5) based on 22 oxygens per formula unit is 5.88, and the mean value for octahedral Al is 0.328 for biotite from the isograd and 0.563 for biotite from the orthoamphibole zone. The Ti-content increases from mean values of 0.199 atoms for biotites in the orthoamphibole zone through 0.351 atoms at the isograd to 0.492 atoms in the orthopyroxene zone (see also Fig. 5). The composition of biotites in the same thin section shows a considerable variation that is dependent on the position of this mineral with respect to garnet. The most Mg-rich (and Ti-poor) biotites were analyzed from inclusions in garnet, while the most Fe-rich (and Ti-rich) biotites occur in the matrix. The bulk chemical control on the compo-

sition of biotite is illustrated by values of $MgO/(MgO + FeO)$ that increase from a mean of 0.72 in garnet-bearing samples (Group 2A in Table 1) to 0.78 in the garnet-free samples (Group 1A in Table 1). These compositional variations are independent of the grade of metamorphism and are similar to those described for biotites from comparable rocks in the orthopyroxene zone (van Reenen, 1983a).

Cordierite is not stable in the orthoamphibole-bearing rocks in the orthoamphibole zone; the analyses in Table 6 are, with one exception (DV1), restricted to samples from the isograd. Cordierite in sample DV1 is present as a reactant. A $MgO/(MgO + FeO)$ value of 0.89 in cordierite from sample DV1 (garnet-free Mg-rich rocks of Group 1A in Table 1) is much higher than the mean value

Table 2. Modal composition (volume percent) of orthoamphibole gneisses

Sample	Garnet	Orthoamphibole	Biotite	Kyanite	Sillimanite	Quartz	Plagioclase	Cordierite	Hypersthene	Ore minerals	Graphite
DV. 23	18	19	17	5		24	20				×
DV. 43	2	12	30	6		31	25				×
DV. 53	5	23	17	7		31	24				×
DV. 2	12	35	25	11		5	23				×
DV. 26	12	25	7			55		×	×		×
M. 447	9	23	13			26	29				×
DV. 47	8	20	19			27	26				×
DV. 49		30	×			31	38				×
DR. 184	32	20				48					×
DV. 22		45	3	9		18	32				×
DV. 1		48	15	10		12	25	×			×
M. 215		37	17	13		14	19				×

× = < 1%

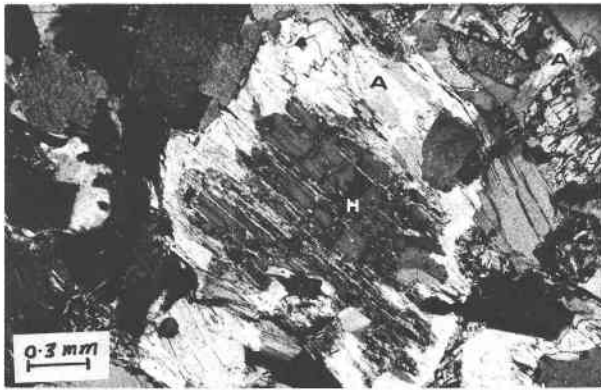


Fig. 6a. Hydration of hypersthene (H) along isograd (sample M346). A = anthophyllite.

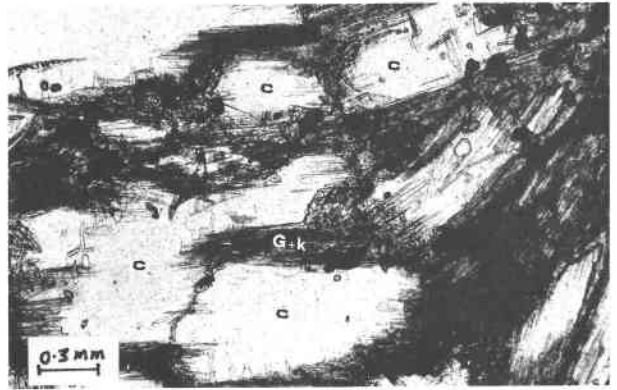


Fig. 6c. Incipient hydration of cordierite in orthopyroxene zone (sample R13). K = kyanite.

of 0.85 for cordierite in the more Fe-rich garnet-bearing rocks (Group 2I, Table 1) from the isograd. This chemical trend is similar to that displayed by biotite and is also in agreement with similar trends described for cordierite from the orthopyroxene zone (van Reenen, 1983a).

All the available analyses for hypersthene are from rocks along the isograd. The Al_2O_3 content of hypersthene in these samples (mean, 3.06 wt%, Table 6) is slightly lower than the mean of 5.89 wt% that was reported for this mineral in similar rocks from the orthopyroxene zone (van Reenen, 1983a). Analyses for adjacent hypersthene and anthophyllite in the same sample on the isograd are identified as such in Tables 6 and 7. The variability in the hypersthene (and orthoamphibole) composition for a specific sample is shown by more than one analysis.

Anthophyllite and gedrite coexist in a variety of textures in the pelitic gneisses in the orthoamphibole zone, and a common occurrence is as large discrete grains with sharp optical contacts (Fig. 7). In this mode of occurrence the two minerals could be distinguished optically—anthophyllite being colorless and gedrite showing faint pleochroism.

Representative analyses for anthophyllite and gedrite, or Al-rich anthophyllite, from rocks along the isograd and

from the orthoamphibole zone are given in Tables 7 and 8. The variability in the orthoamphibole composition for a specific sample is shown by more than one analysis. The accuracy of these analyses has been evaluated using the "residual value" method of Robinson et al. (1971). This method is based on an ideal formula $\text{Na}_x\text{R}_2^{3+}(\text{R}_2^{3+}, \text{R}_3^{3+})(\text{Al}_{x+y}\text{Si}_{8-x-y})\text{O}_{22}(\text{OH})_2$, where x = A occupancy and y = octahedral Al + Fe^{3+} + Cr^{3+} + 2Ti^{4+} . Substitutions of Na (and K) in the A site (x) and of R^{3+} in the octahedral sites (y) are compensated by substitution of Al for Si in the tetrahedral sites, so that the sum of x and y must be equal to the amount of tetrahedral Al as shown in the ideal formula (Robinson et al., 1971, p. 1010). The "residual value" is $(x + y) - \text{Al}^{\text{IV}}$, and this value has a mean of -0.062 (with a range from -0.140 to $+0.044$) for anthophyllites, and a mean of $+0.078$ (with a range from -0.07 to $+0.234$) for gedrites in this study. These small values compare favorably with other orthoamphibole analyses in the literature (e.g., Grant, 1981, p. 1129) and indicate either analytical error or small deviations from the ideal formula. The classification of the orthoamphiboles from this study into anthophyllite, Al-rich anthophyllite and gedrite is shown in Figure 8.

The gedrites from the isograd differ markedly in com-



Fig. 6b. Hydration of cordierite (C) along isograd (sample M346). G = gedrite.

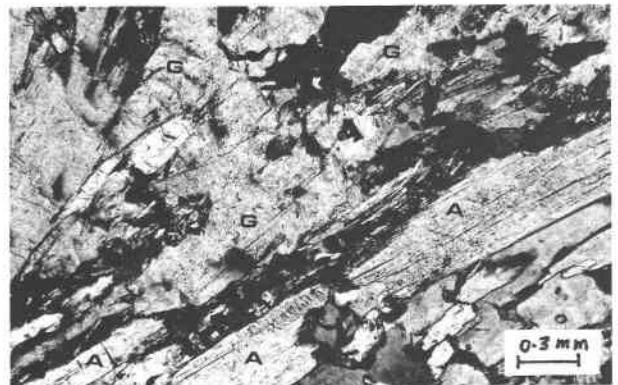


Fig. 7. Coexisting high-Al gedrite (G) and low-Al anthophyllite (A) in orthoamphibole zone.

Table 3. Chemical analyses of orthoamphibole gneisses from isograd (DV3 to DV38) and orthoamphibole zone (DV43 to DR184)

Sample	DV. 3	DR. 157	DV. 38	DV. 43	M. 447	DV. 22	DV. 1	DR. 184
SiO ₂	65.20	55.23	57.70	65.40	57.26	57.40	65.36	49.97
Al ₂ O ₃	13.70	18.50	14.70	14.30	16.96	14.70	13.84	13.98
Fe ₂ O ₃	0.88	0.73	3.0	0.74	2.50	1.17	1.07	1.15
FeO	7.92	8.88	10.80	6.66	6.56	10.53	4.90	17.76
MgO	6.30	8.86	7.60	5.50	7.13	9.50	7.55	10.39
MnO	0.08	0.10	0.12	0.10	0.11	0.16	0.05	0.20
CaO	1.39	0.68	1.99	1.95	2.13	1.78	1.87	1.68
Na ₂ O	1.80	0.81	2.50	2.60	2.34	2.20	2.40	0.66
K ₂ O	1.82	2.25	1.98	1.86	1.18	0.29	0.23	0.52
TiO ₂	0.68	0.82	0.66	0.58	0.67	0.92	0.58	0.66
P ₂ O ₅	0.05	0.07	0.11	0.09	0.05	0.19	0.08	0.11
H ₂ O ⁺	0.80	1.14	0.90	0.90	1.69	0.80	1.06	1.46
CO ₂	0.30	0.90			0.19	0.30	0.09	0.69
H ₂ O ⁻	0.12	0.20	0.46	0.49	0.28	0.73	0.15	0.26
Total	101.04	99.26	102.52	101.17	99.05	100.67	99.23	99.49

The mineralogical subdivision of these samples are given in Table 1

position from gedrite in chemically similar samples from the orthoamphibole zone. They are much more aluminous (Al₂O₃ = 18.42–20.68 wt%) than gedrite from the orthoamphibole zone (Al₂O₃ = 13.87–16.00 wt%) and are also characterized by higher Na₂O contents (1.81–2.27 wt% against 1.00–1.43 wt%). The gedrites from the isograd (and especially those from sample DV3) have the highest Al₂O₃ content (20.68 wt%) of any orthoamphiboles reported in the literature (e.g., Rabbitt, 1948; Robinson and Jaffe, 1969; Robinson et al., 1971; Lal and Moorhouse, 1969; Gable and Sims, 1969; Beeson, 1978; Spear, 1980). The high Na₂O content (2.27 wt%) of this gedrite is similar to the values of 2.27–2.38 wt% reported for gedrites in sample 73-29D of Spear (1980) and 2.30 wt% for gedrite of analysis G-23 in Grant (1981).

The gedrites (and anthophyllites) from the orthoam-

phibole zone are also enriched in Fe as compared to those from chemically similar rocks along the isograd. It is therefore reasonable to suggest that the observed differences in the composition of gedrites are due only to differences in metamorphic conditions. The compositions of anthophyllites from the isograd do not show significant differences with respect to their Na₂O and Al₂O₃ contents when compared to those from the orthoamphibole zone, although there is a slight increase in Al₂O₃ and Na₂O in anthophyllites within this zone.

The presence of a miscibility gap in the anthophyllite-gedrite series is well documented in the literature (Robinson et al., 1971; Spear, 1980) and coexisting subsolvus orthoamphiboles have been described by Stout (1970, 1971, 1972), Robinson et al. (1982), Spear (1978, 1980, 1982), and van Reenen (1983b). Figure 9 is a plot of A-site

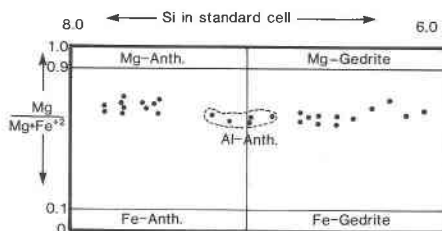


Fig. 8. Classification of orthoamphiboles in the present study after Leake (1978).

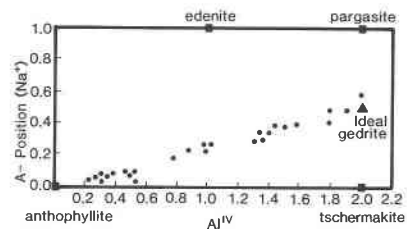


Fig. 9. Plot of A-site occupancy vs. Al^{IV} for all available orthoamphibole analyses.

Table 4. Representative electron-microprobe analyses of garnet

	DV.38 Core	DV.38 Rim	DR.157	DV.3	DV.43	M.447 Core	M.447 Rim	DR.184 Core	DR.184 Rim
SiO ₂	39.25	39.33	40.57	40.06	39.39	38.31	38.30	38.34	38.15
Al ₂ O ₃	22.35	22.39	21.93	22.28	22.19	21.68	21.78	22.40	22.06
MgO	9.06	9.11	7.93	7.31	5.56	6.95	6.54	7.00	5.91
FeO	27.68	28.65	27.45	29.77	30.79	30.21	29.33	30.28	32.53
CaO	2.09	1.15	1.14	1.27	2.00	1.64	2.81	2.76	2.01
MnO	0.33	0.29	0.60	0.56	1.27	1.16	1.03	0.31	0.32
Na ₂ O	-	-	0.01	-	0.01	-	-	-	0.01
Cr ₂ O ₃	0.14	0.16	0.05	0.14	0.27	0.13	0.16	0.11	2.01
Total	100.90	101.09	99.66	101.39	101.48	100.08	99.95	101.20	101.27
Cations per 24 oxygens									
Si	5.99	6.0	6.22	6.11	6.08	5.99	5.99	5.92	5.94
Al ^{iv}	0.01	0.01	-	-	-	0.01	0.01	0.08	0.06
	6.0	6.01	6.22	6.11	6.08	6.0	6.0	6.0	6.0
Al ^{vi}	4.01	4.02	3.97	4.01	4.04	3.99	4.01	4.0	3.99
Mg	2.06	2.07	1.81	1.66	1.28	1.62	1.52	1.61	1.37
Fe	3.53	3.65	3.52	3.8	3.97	3.95	3.84	3.91	4.33
Ca	0.34	0.19	0.19	0.21	0.33	0.28	0.47	0.46	0.34
Mn	0.04	0.04	0.08	0.07	0.17	0.15	0.14	0.04	0.04
Na	-	-	0.01	-	0.01	-	-	-	0.00
Cr	0.02	0.02	0.01	0.02	0.03	0.02	0.02	0.01	0.04
	5.99	5.97	5.62	5.76	5.78	6.02	5.99	6.03	6.02
Mg/Mg+Fe ⁺²	.37	0.36	0.34	0.30	0.24	0.29	0.28	0.29	0.25

occupancy vs. Al^{iv} for all the available anthophyllite (including Al-rich anthophyllite) and gedrite analyses from this study. The linear trend observed in this diagram is identical to that reported by Robinson and Jaffe (1969), Robinson et al. (1971, 1982), James et al. (1978), Spear (1980), and Grant (1981). The trend from anthophyllite to gedrite is very pronounced and is toward the composition of "ideal" gedrite as defined by Robinson et al. (1971). The significance of Al-rich anthophyllite in Figures 8 and 9 is unclear. All three amphiboles were identified as discrete (although not touching) grains in sample DV1 (see Tables 7, 8) and subsequently also in sample DR157 from the isograd. Al-rich anthophyllite coexists with gedrite in sample DR157, but was not found in contact with anthophyllite.

The miscibility gap between anthophyllite and gedrite is also clearly illustrated in Figure 10. It is manifested by a large discontinuity in the A-site occupancy and in the

Al^{iv} and Al^{vi} contents (Spear, 1980, p. 1109). The dependence of the size and shape of the miscibility gap in terms of X_{Fe} with respect to A-site occupancy and Al^{iv} is obvious from Figure 10. The widening of this gap in more Mg-rich compositions, however, is not in agreement with Spear's data (Robinson et al., 1982, p. 66 and Fig. 29), which showed that the gap should be narrower for Mg-rich compositions and also that the solvus would close off in Mg-rich compositions at a lower temperature than in Fe-rich compositions. The Mg-rich compositions from this study are from the isograd (Group 2I, Table 1), and the Fe-rich compositions are from chemically similar lower-grade rocks (Group 2A, Table 1) from the orthoamphibole zone.

The distribution of Fe and Mg between coexisting anthophyllite and gedrite from this study (Fig. 10) is very similar to that described by Spear (1980) for coexisting orthoamphiboles from the Post Pond Volcanics in Ver-

Table 5. Representative electron-microprobe analyses of biotite

	DV.38 ^{-1*}	DV.38	DR.157	DV.3	DV.1	DV.43	M.447	DV.22
SiO ₂	36.93	37.54	37.97	37.53	38.99	37.91	39.64	37.95
Al ₂ O ₃	17.04	17.08	17.06	17.49	17.59	18.42	17.87	17.68
TiO ₂	3.07	3.54	3.20	3.68	1.74	1.82	1.73	1.47
MgO	17.91	17.17	17.37	17.06	18.11	16.42	16.76	17.47
FeO	11.11	11.47	11.67	11.64	8.99	12.70	11.61	11.37
CaO	-	-	-	-	0.01	-	0.02	0.01
MnO	-	-	-	-	-	0.02	0.03	0.03
Na ₂ O	0.45	0.29	0.37	0.28	0.50	0.53	0.50	0.44
K ₂ O	9.32	9.29	9.38	9.89	8.35	8.56	8.96	8.36
Cr ₂ O ₃	0.50	0.52	0.43	0.76	0.52	0.46	0.29	0.40
Total	96.32	96.91	97.45	98.32	94.79	96.84	95.40	95.20
Cations per 22 oxygens								
Si	5.36	5.41	5.45	5.36	5.62	5.46	5.49	5.52
Al ^{iv}	2.64	2.59	2.56	2.64	2.38	2.54	2.51	2.48
	8.0	8.0	8.0	8.0	8.0	8.0	8.0	8.0
Al ^{vi}	0.28	0.31	0.33	0.30	0.61	0.59	0.57	0.56
Ti	0.34	0.38	0.35	0.40	0.19	0.20	0.19	0.16
Mg	3.87	3.69	3.71	3.63	3.89	3.52	3.65	3.79
Fe	1.35	1.38	1.40	1.39	1.08	1.53	1.42	1.38
Cr	0.06	0.06	0.05	0.09	0.06	0.05	0.03	0.05
	5.90	5.82	5.84	5.81	5.83	5.89	5.86	5.94
Na	0.13	0.08	0.10	0.08	0.14	0.15	0.14	0.12
K	1.73	1.71	1.72	1.80	1.54	1.57	1.67	1.55
	1.86	1.79	1.82	1.88	1.68	1.72	1.81	1.67
Mg/Mg+Fe ⁺²	0.74	0.73	0.73	0.72	0.78	0.7	0.72	0.73

* In contact with garnet. The rest are from the matrix

mont: gedrite is enriched in Fe relative to coexisting anthophyllite. Total Fe varies very little between anthophyllite and coexisting gedrite, whereas anthophyllite is always enriched in Mg relative to gedrite. A similar relationship in the orthoamphiboles has been described by Kamineni (1975), Spear (1980, Fig. 9), and Grant (1981).

The observed regularity of compositions of minerals such as garnet, biotite, and orthoamphiboles across the retrograde isograd implies that mineral assemblages are in a close approach to chemical equilibrium along the

isograd. This is substantiated by the repeated presence along the isograd of both the reactants and the products (hypersthene + anthophyllite + quartz, and cordierite + gedrite + kyanite + quartz) of the hydration reactions in the same samples.

PHASE RELATIONS

The analytical data from Table 3 and Tables 4 to 8 are illustrated in A'FM diagrams (Fig. 11), where A' = Al₂O₃-K₂O-CaO-Na₂O, F = total iron as FeO, and M =

Table 6. Representative electron-microprobe analyses of cordierite and hypersthene

Cordierite				Hypersthene						
	DR. 157	DV. 3	DV. 1	DR. 157	DR. 157 ⁺	DV. 3 ⁺	DV. 3	DV. 38 ⁺	DV. 38	
SiO ₂	48.96	48.76	49.18	52.87	51.69	51.12	51.84	52.61	51.63	
Al ₂ O ₃	33.21	32.81	33.22	3.04	3.45	2.87	2.53	3.29	3.18	
MgO	11.51	10.73	11.92	0.04	0.02	0.02	0.02	-	0.02	
FeO	3.00	3.83	2.60	24.49	22.22	22.15	21.30	23.97	23.15	
MnO	0.03	0.02	0.01	21.97	22.77	23.61	25.37	21.53	21.40	
Na ₂ O	0.11	0.10	0.13	CaO	0.08	0.05	0.08	0.10	0.09	
				MnO	0.19	0.22	0.21	0.19	0.08	
				Na ₂ O	0.01	0.01	-	-	-	
				Cr ₂ O ₃	0.11	0.17	0.28	0.20	0.14	
Total	96.82	96.25	97.07	Total	102.80	100.61	100.34	101.57	101.71	
Cations per 18 oxygens				Cations per six oxygens						
Si	4.99	5.02	5.0	Si	1.91	1.91	1.91	1.93	1.91	
Al	3.99	3.98	3.98	Al ^{iv}	0.09	0.09	0.09	0.08	0.09	
Mg	1.75	1.65	1.81		2.0	2.00	2.00	2.00	2.00	
Fe	0.26	0.33	0.22							
Ca	-	-	-	Al ^{vi}	0.04	0.06	0.04	0.04	0.05	
Na	0.02	0.02	0.03	Mg	1.29	1.23	1.23	1.20	1.30	
				Fe	0.68	0.71	0.74	0.76	0.66	
				Mn	0.01	0.01	0.01	0.01	0.01	
				Cr	-	0.01	0.01	0.01	-	
	11.01	11.00	11.04		2.02	2.02	2.03	2.02	2.02	
Mg/Mg+Fe	0.87	0.83	0.89	Mg/Mg+Fe ⁺²	0.67	0.64	0.63	0.60	0.67	

* Indicate grains in contact with anthophyllite in Table 4d.

MgO. Small amounts of K-feldspar can occur in assemblages from the orthopyroxene zone (Table 1; van Reenen, 1983a, Table 1), but this mineral was never recognized in orthoamphibole-bearing assemblages (Table 2). Ac-

cordingly, most of the minerals in the pelitic rocks of this study can be expressed in A'FM diagrams, which illustrate the dependence of assemblages on the Fe/Mg ratio of the rocks (see also Grant, 1981, p. 1129). Biotite has been omitted from these diagrams because it lies out of the AFM plane owing to Ti substitution (Table 5; van Reenen, 1983a, Table 4d).

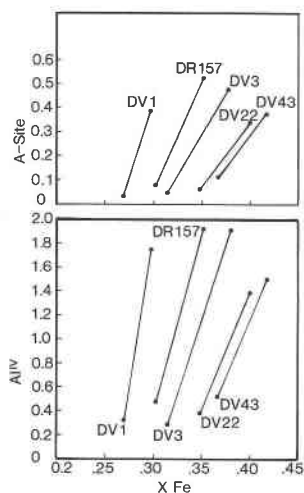


Fig. 10. A-site occupancy and Al^{iv} vs. X_{Fe} for coexisting gedrite and anthophyllite.

Initial phase relations before hydration

Mineral assemblages in metapelitic gneisses from the orthopyroxene zone represent the initial conditions associated with isothermal uplift (M2) before the establishment of the retrograde isograd during M3 (Fig. 3). The general phase relations in these metapelitic granulites [with MgO/(MgO + FeO) = 0.59 - 0.70, Group 2P in Table 1] are illustrated in Figure 11a. The tie lines in this diagram connect the actual compositions of the coexisting minerals in six representative samples from widely different areas in this metamorphic zone (van Reenen, 1983a, Fig. 5). The chemographic relations in this diagram illustrate the continuous Fe-Mg reaction garnet + quartz = cordierite + hypersthene, which is petrographically expressed by the presence of corona textures (van Reenen, 1983a: Figs. 3b, 3c, 3d, 4a). This reaction records con-

Table 7. Representative electron-microprobe analyses of anthophyllite

	DV.38 [†]	DR.157 [†]	DR.157	DV.3 [†]	DV.1	DV.43	DV.22
SiO ₂	53.02	54.41	53.75	54.19	54.55	51.83	52.94
Al ₂ O ₃	3.99	3.15	3.96	2.47	3.36	4.89	3.67
TiO ₂	0.08	0.03	0.04	0.02	0.07	0.11	0.11
MgO	22.10	22.72	23.43	22.27	22.96	19.51	20.33
FeO	17.85	17.96	17.57	18.15	15.06	20.17	19.46
CaO	0.21	0.16	0.20	0.16	0.24	0.25	0.30
MnO	0.08	0.14	0.16	0.09	0.12	0.27	0.23
Na ₂ O	0.29	0.22	0.27	0.17	0.22	0.38	0.21
Cr ₂ O ₃	0.17	0.16	0.16	0.20	0.42	0.14	0.17
Total	97.79	98.96	99.54	97.72	97.0	97.55	97.42
Cations per 23 oxygens							
Si	7.54	7.63	7.49	7.70	7.7	7.48	7.61
Al ^{iv}	0.46	0.37	0.51	0.30	0.30	0.52	0.39
	8.0	8.0	8.0	8.0	8.0	8.0	8.0
Al ^{vi}	0.20	0.15	0.14	0.12	0.25	0.31	0.23
Mg	4.68	4.75	4.87	4.72	4.83	4.20	4.36
Fe	2.12	2.11	2.05	2.16	1.78	2.43	2.34
Ti	0.01	-	0.01	-	0.01	0.01	0.01
Cr	0.02	0.02	0.02	0.02	0.05	0.02	0.02
Ca	0.03	0.02	0.03	0.02	0.04	0.04	0.05
Mn	0.01	0.02	0.02	0.02	0.01	0.03	0.03
M ₁ -M ₄	7.08	7.07	7.14	7.06	7.00	7.04	7.04
Na (A)	0.08	0.06	0.07	0.05	0.06	0.11	0.06
Mg/Mg+Fe ⁺²	0.69	0.69	0.70	0.69	0.73	0.63	0.65

[†]Indicate grains in contact with hypersthene in Table 4c.

ditions of essentially isothermal ($T = 800^{\circ}\text{C}$) uplift (M2, Fig. 3) that raised crustal blocks from depths of at least 35 km (10 kbar) to 23 km (7 kbar, van Reenen, 1983a). This same reaction has run to completion in samples with $\text{MgO}/(\text{MgO} + \text{FeO}) > 0.70$ (Group 1P in Table 1), thereby giving rise to assemblages of cordierite + hypersthene + biotite (+ quartz + plagioclase) without garnet.

Final phase relations after hydration

The orthopyroxene- and cordierite-free assemblages (Fig. 11b), which represent the final conditions in the orthoamphibole zone after hydration, are characterized by the presence of coexisting anthophyllite + gedrite + kyanite (+ quartz + plagioclase + biotite) in MgO-rich rocks [$\text{MgO}/(\text{MgO} + \text{FeO}) > 0.59$, Table 1]. Figure 11b also illustrates the influence of the MgO/FeO ratio of the rocks on the composition of coexisting minerals in the orthoamphibole-bearing gneisses. This is shown by comparing the phase relations in sample DV1 [$\text{MgO}/(\text{MgO} + \text{FeO}) > 0.7$, Group 1A in Table 1] with those of samples DV22 and DV43 [$\text{MgO}/(\text{MgO} + \text{FeO}) = 0.59\text{--}0.70$, Group 2A

in Table 1]. Garnet is also absent from the MgO-rich rocks (DV1, Fig. 11b), whereas the FeO-rich assemblages (DR184, Fig. 11b) contain only garnet, gedrite, and quartz.

Phase relations on the retrograde isograd

Two important mineral assemblages that were recognized along the isograd in relatively Al-poor metapelitic gneisses are shown in Figure 11c: garnet + hypersthene + anthophyllite + quartz + plagioclase (+ biotite) in FeO-rich and Al₂O₃-poor bulk compositions with $\text{MgO}/(\text{MgO} + \text{FeO}) < 0.59$ (DV38, Group 3I in Table 1), and the apparent low-variance assemblage of hypersthene + anthophyllite + gedrite + cordierite + kyanite + quartz + plagioclase (+ biotite) in more MgO- and Al₂O₃-rich bulk compositions with $\text{MgO}/(\text{MgO} + \text{FeO}) > 0.59$ (DV3 and DR157, Group 2I in Table 1). These minerals occur in the same thin section, but not in direct contact with each other. Cordierite is intergrown with gedrite and kyanite (Fig. 6b), and hypersthene is partly or completely surrounded by anthophyllite (Fig. 6a). The following sub-assemblages (in addition to plagioclase and biotite) are

Table 8. Representative electron-microprobe analyses of Al-rich anthophyllite (first two) and gedrite

	DV. 1	DR. 184	DR. 157	DR. 157	DV. 3	DV. 1	DV. 43	M. 447	DV. 22	DV. 22	DR. 184
SiO ₂	49.11	46.68	41.65	44.54	42.45	43.73	45.15	44.28	46.18	46.34	45.62
Al ₂ O ₃	10.14	11.05	20.58	18.42	20.68	19.64	15.45	16.06	14.63	13.87	13.09
TiO ₂	1.01	0.06	0.17	0.19	0.04	-	0.23	0.46	0.09	0.08	0.49
MgO	19.56	17.11	16.56	17.37	15.19	17.76	15.53	15.95	16.56	16.68	16.17
FeO	15.58	19.72	15.79	16.85	16.53	13.41	19.87	18.18	19.77	19.05	19.61
CaO	0.34	0.42	0.21	0.27	0.14	0.25	0.41	0.37	0.29	0.34	0.49
MnO	0.13	0.05	0.15	0.15	0.10	0.14	0.31	0.27	0.30	0.28	0.06
Na ₂ O	0.86	0.93	2.23	1.81	2.27	1.76	1.42	1.43	1.29	1.25	1.00
Cr ₂ O ₃	0.75	0.15	0.06	0.02	0.02	-	0.17	0.32	0.17	0.13	0.26
Total	97.50	96.16	97.41	99.63	97.43	96.69	98.55	97.32	99.28	98.03	96.80
Cations per 23 oxygens											
Si	6.97	6.86	5.97	6.24	6.09	6.21	6.49	6.41	6.57	6.66	6.66
Al ^{iv}	1.03	1.14	2.03	1.76	1.91	1.79	1.51	1.59	1.43	1.34	1.34
	8.0	8.0	8.0	8.0	8.0	8.0	8.0	8.0	8.0	8.0	8.0
Al ^{vi}	0.67	0.77	1.45	1.29	1.58	1.50	1.11	1.14	1.03	1.01	0.92
Mg	4.16	3.75	3.54	3.63	3.25	3.76	3.33	3.44	3.51	3.57	3.52
Fe	1.86	2.42	1.90	1.98	1.98	1.59	2.39	2.20	2.35	2.29	2.40
Ti	0.11	0.01	0.02	0.02	0.01	-	0.03	0.05	0.01	0.01	0.05
Cr	0.08	0.02	0.01	-	-	-	0.02	0.03	0.02	0.02	0.03
Ca	0.05	0.07	0.03	0.04	0.02	0.04	0.06	0.06	0.04	0.05	0.08
Mn	0.02	0.01	0.02	0.02	0.01	0.02	0.04	0.03	0.04	0.03	0.01
M ₁ -M ₄	7.00	7.05	7.0	6.99	6.85	6.91	6.98	6.95	7.0	6.98	7.01
Na (A)	0.24	0.27	0.62	0.49	0.63	0.49	0.40	0.40	0.36	0.35	0.28
Mg/Mg+Fe ⁺²	0.69	0.61	0.65	0.65	0.62	0.70	0.58	0.61	0.60	0.61	0.60

recognized: hypersthene + anthophyllite + gedrite + quartz, cordierite + gedrite + kyanite + quartz, and cordierite + gedrite + anthophyllite + quartz. The presence of a possible low-variance assemblage in MgO-rich rocks on the isograd (gedrite + anthophyllite + cordierite + kyanite + quartz) is indicated by the dashed tie line between anthophyllite and kyanite in Figure 11c. Garnet is present in the more FeO-rich assemblages, but is probably absent in the more MgO-rich assemblages. This is indicated by the absence of tie lines between garnet and the other minerals in the latter rock type.

METAMORPHIC CONDITIONS

Metamorphic temperatures at the isograd and in the orthoamphibole zone can firstly be estimated by comparing published information on the solvus in the orthoamphibole system to the results of the present study.

The orthoamphibole-bearing assemblages from the orthoamphibole zone have some important distinctions when compared with similar rocks from elsewhere. Medium-

grade assemblages high in the kyanite-staurolite zone and low in the sillimanite-staurolite-muscovite zone ($T = \sim 530\text{--}550^\circ\text{C}$, Spear, 1980) from central Massachusetts are characterized by the absence of coexisting orthoamphibole \pm kyanite \pm sillimanite (Robinson et al., 1982, Fig. 87). Sillimanite coexists with gedrite in higher-grade assemblages ($T = 625\text{--}650^\circ\text{C}$, Spear, 1980, p. 1116) from the middle of the sillimanite-muscovite-staurolite zone from "Amphibole Hill," southwestern New Hampshire, but the orthoamphiboles were above the orthoamphibole solvus (Robinson et al., 1971).

The orthoamphibole-bearing assemblages from the retrograde isograd show similarities with samples from the sillimanite-orthoclase zone ($650\text{--}675^\circ\text{C}$) of central Massachusetts (Robinson and Tracy, 1979, in Robinson et al., 1982, Fig. 99) where gedrite coexists with hypersthene and garnet in fairly FeO-rich rocks. Anthophyllite is present within gedrite as a few colorless patches in sharply defined contact with the gedrite host (Robinson et al., 1982, p. 190). The coexistence of hypersthene and silli-

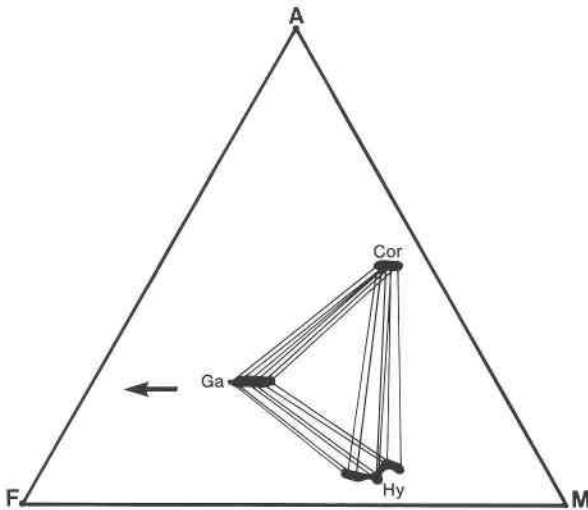


Fig. 11a. Topology of the reaction garnet (Ga) + quartz = cordierite (Cor) + hypersthene (Hy) shown in an A'FM diagram. Arrow indicates direction of reaction toward Fe enrichment during M2 isothermal uplift.

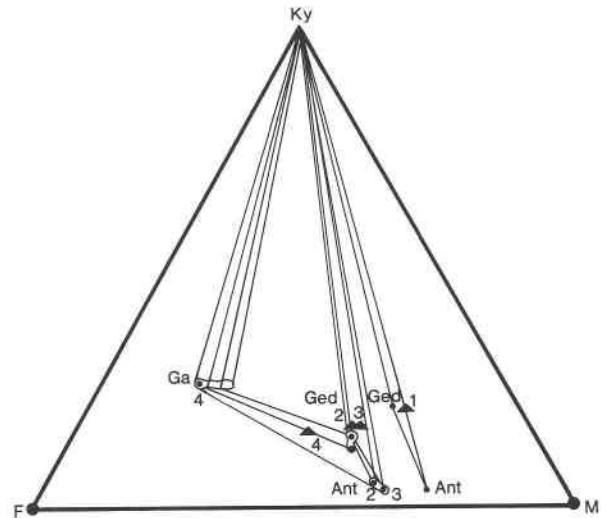


Fig. 11b. Chemographic relations of the phases anthophyllite (Ant), gedrite (Ged), kyanite (Ky), and garnet (Ga) in the orthoamphibole zone as shown in an A'FM diagram. Garnet unstable in Mg-rich compositions. 1 = DV1, 2 = DV43, 3 = DV22, 4 = DR184, \blacktriangle = composition of sample.

manite in this rock type is excluded by the tie line between gedrite and garnet. Although coexisting gedrite + anthophyllite + hypersthene (which is restricted to the retrograde isograd in the present study) is not described from this locality, it should be a stable assemblage in samples with a restricted bulk composition (Robinson et al., 1982, Fig. 99).

The orthoamphibole-bearing assemblages in the sillimanite-orthoclase zone of central Massachusetts formed under conditions about 50 deg higher than the suite of entirely hypersolvus orthoamphiboles studied from the "Amphibole Hill" area from southwestern New Hampshire (Robinson et al., 1982, p. 190). The opening of the orthoamphibole solvus at these high temperatures is ascribed to the high Ti content of the gedrite (with 0.10 Ti per formula unit), and the presence of anthophyllite patches in gedrite are described as relicts from a prograde reaction anthophyllite + garnet = orthopyroxene + gedrite + H₂O (Robinson et al., 1982, p. 190). The presence of an orthoamphibole solvus in samples from the retrograde isograd in the southern marginal zone, however, cannot be explained by a high Ti content of these gedrites (maximum Ti content of gedrite less than 0.05 Ti per formula unit). It is possible, therefore, that the metamorphic temperatures along the retrograde isograd might be lower than the estimate (625–650°C) for "Amphibole Hill" (Spear, 1980, p. 1116).

The presence of kyanite in the orthoamphibole-bearing gneisses at the isograd (Fig. 6b) and in the orthoamphibole zone (Figs. 4b, 4c) supports the temperature estimate of less than 625–650°C for the metamorphic conditions based on the presence of the orthoamphibole solvus. This implies a minimum pressure of ~6 kbar if Holdaway's (1971) Al₂SiO₅-phase diagram is used (Fig. 3). These conditions

support the presence of a systematic temperature gradient in the southern marginal zone of the Limpopo belt after rapid uplift (M2) and during the M3 hydrating event (Fig. 3). Isobaric cooling from M2 (Fig. 3) gives a temperature (based on the presence of kyanite) of more than 700°C, which is about 100 deg higher than the crest of the solvus in the orthoamphibole system (600 ± 25°C) as defined by Spear (1980, Fig. 14).

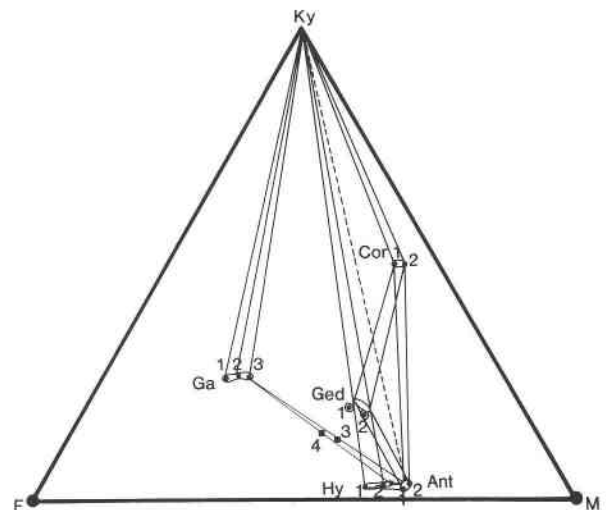


Fig. 11c. Chemographic relations of the phases cordierite (Cor), gedrite (Ged), kyanite (Ky), anthophyllite (Ant), garnet (Ga), and hypersthene (Hy) on the isograd, as shown in an A'FM diagram. Garnet unstable in Mg-rich compositions (DV3, DR157), as indicated by absence of tie lines. 1 = DV3, 2 = DR157, 3 = DV38, 4 = DV34; \blacksquare and \circ = composition of samples; other symbols as in Figs. 11a and 11b.

Metamorphic temperatures in the different zones (including the orthopyroxene zone) were also estimated with the garnet-biotite thermometer (Ferry and Spear, 1978). The partitioning of Fe and Mg between biotite (in the matrix) and the rim composition of garnet yielded temperatures that changed systematically from the orthopyroxene zone (mean value for 10 pairs, 810°C; range, 740–890°C) through the isograd (mean value for 5 pairs, 640°C; range, 610–680°C) to the orthoamphibole zone (mean value for 8 pairs, 530°C; range, 510–570°C). These estimations cannot be seen as cooling temperatures because the presence of a systematic temperature gradient (Fig. 3) suggests fluid flow at a fixed temperature during hydration. The temperature of 810°C for the orthopyroxene zone, based on the garnet-biotite geothermometer, also agrees with calculated temperatures of ~800°C based on other methods (van Reenen, 1983a).

The estimated temperature of less than about 625–650°C for the metamorphic conditions on the retrograde isograd is far below the upper thermal stability limit of anthophyllite in quartz-bearing rocks (>750°C at pressures >3 kbar, Greenwood, 1963) under conditions where the water pressure equals the total pressure. It follows that the water pressure must have been much lower than the total pressure during the hydration of cordierite and hypersthene.

FLUID COMPOSITION ON THE ISOGRAD

Evidence has been presented that anthophyllite, hypersthene, and quartz might be in equilibrium in metapelitic gneisses along the retrograde isograd. The anthophyllite breakdown reaction may therefore be used to estimate the maximum fluid composition under conditions where $P_f = P_{\text{total fluid}}$. The calculated equilibrium curve anthophyllite = 7 enstatite + quartz + water, based on the data of Helgeson et al. (1978), is shown as the solid line in Figure 3. Also shown on this figure is the box (M3) representing the P - T estimates for the isograd assemblages. In order to displace the calculated equilibrium curve to the P - T box, the fugacity of H_2O must be lowered. The amount of lowering can be accomplished by diluting the mole fraction of H_2O in the fluid phase to a value of about 0.2, as calculated using a modified Redlich-Kwong equation of state for nonideal mixing of H_2O and CO_2 (Holloway, 1977; Flowers, 1979).

CONCLUSIONS

The M3 retrograde orthoamphibole isograd in the southern marginal zone of the Limpopo belt is expressed in Mg-rich pelitic gneisses by two hydration reactions that are superimposed on M2 corona textures of cordierite and hypersthene after garnet: hypersthene + quartz + H_2O = anthophyllite, and cordierite + H_2O = gedrite + kyanite + quartz. Anthophyllite + hypersthene + quartz coexist at a temperature of less than 625–650°C and a minimum pressure of 6 kbar in a narrow zone defined by the retrograde isograd, whereas chemically similar, but completely retrogressed and recrystallized rocks south of the

isograd are characterized by the presence of coexisting orthoamphiboles and kyanite.

The estimated temperature of hydration for the isograd is far below the upper thermal stability limit of anthophyllite in quartz-bearing rocks under conditions where the water pressure equals the total pressure. A modified Redlich-Kwong equation of state for nonideal mixing of H_2O and CO_2 was used to calculate the mole fraction of H_2O of about 0.2 in the fluid phase necessary to displace the equilibrium curve anthophyllite = 7 enstatite + quartz + water to the estimated P - T condition on the isograd (Fig. 3). The CO_2 -rich retrograde fluid infiltrated toward the end of the Limpopo tectonothermal event while the rocks in the southern marginal zone still had a temperature gradient (Fig. 3). This retrograde event either accompanied, or closely followed, the emplacement of the Matok charnockitic-granitic pluton at 2620 Ma (Fig. 2; Du Toit et al., 1983). The results of a fluid-inclusion study across the isograd and possible sources of the CO_2 -rich hydrating fluid will be discussed in a paper under preparation.

ACKNOWLEDGMENTS

This study forms part of the South African National Geodynamics Project, and the financial support of the CSIR is gratefully acknowledged. Special thanks are also due to the Anglo American Research Laboratories in Johannesburg for permission to use their microprobe facilities. I thank Cornelis Klein for his critical comments on an early draft of this paper and Takashi Miyano for performing the thermodynamic calculations while on leave from the University of Tsukuba, Japan. I am also grateful to J. M. Rice and J. A. Grant for their constructive reviews that improved the manuscript considerably. Special thanks go to Lincoln Hollister for his time and energy in the field and for his critical comments on the final draft of the manuscript. Elsa Maritz typed the manuscript and the figures were drafted by N. Maree.

REFERENCES

- Barton, J.M., Jr., Du Toit, M.C., van Reenen, D.D., and Ryan, B. (1983) Geochronological studies in the southern marginal zone of the Limpopo mobile belt, southern Africa. Geological Society of South Africa Special Publication, 8, 55–64.
- Beeson, R. (1978) The geochemistry of orthoamphiboles and coexisting cordierites and phlogopites from south Norway. Contributions to Mineralogy and Petrology, 66, 5–14.
- Du Toit, M.C., and van Reenen, D.D. (1977) The southern margin of the Limpopo mobile belt, northern Transvaal, with special reference to metamorphism and structure. Geological Survey of Botswana Bulletin, 12, 83–97.
- Du Toit, M.C., van Reenen, D.D., and Roering, C. (1983) Some aspects of the geology structure and metamorphism of the southern marginal zone of the Limpopo metamorphic complex. Geological Society of South Africa Special Publication, 8, 121–142.
- Ferry, J.M., and Spear, F.S. (1978) Experimental calibration of the partitioning of Fe and Mg between biotite and garnet. Contributions to Mineralogy and Petrology, 66, 113–117.
- Flowers, G.C. (1979) Correction of Holloway's (1977) adaptation of the modified Redlich-Kwong equation of state for calculation of the fugacities of molecular species in supercritical fluids of geologic interest. Contributions to Mineralogy and Petrology, 69, 315–318.

- Gable, D.J., and Sims, P.K. (1969) Geology and regional metamorphism of some high-grade cordierite gneisses, Front Range, Colorado. Geological Society of America Special Paper 128, 87 p.
- Grant, J.A. (1981) Orthoamphibole and orthopyroxene relations in high-grade metamorphism of pelitic rocks. *American Journal of Science*, 281, 1127–1143.
- Greenwood, H.J. (1963) Synthesis and stability of anthophyllite. *Journal of Petrology*, 4, 317–351.
- Helgeson, H.C., Delany, J.M., Nesbitt, H.W., and Bird, D.K. (1978) Summary and critique of the thermodynamic properties of rock-forming minerals. *American Journal of Science*, 278-A, 1–229.
- Holdaway, M.J. (1971) Stability of andalusite and the aluminium silicate phase diagram. *American Journal of Science*, 271, 97–131.
- Holloway, J.R. (1977) Fugacity and activity of molecular species in supercritical fluids. In D.G. Fraser, Ed. *Thermodynamics in geology*, 161–181. Reidel, Dordrecht, The Netherlands.
- James, R.A., Grieve, R.A.F., and Pauk, L. (1978) The petrology of cordierite-anthophyllite gneisses and associated mafic and pelitic gneisses at Manitouwadge, Ontario. *American Journal of Science*, 278, 41–63.
- Kamineni, D.C. (1975) Chemical mineralogy of some cordierite-bearing rocks near Yellowknife, Northwest Territories, Canada. *Contributions to Mineralogy and Petrology*, 53, 293–310.
- Lal, R.K., and Moorhouse, W.W. (1969) Cordierite-gedrite rocks and associated gneisses of Fishtail Lake, Harcourt Township, Ontario. *Canadian Journal of Earth Sciences*, 6, 145–165.
- Leake, B.E. (1978) Nomenclature of amphiboles. *American Mineralogist*, 63, 1023–1053.
- Mason, R. (1973) The Limpopo mobile belt, southern Africa. *Royal Society (London) Philosophical Transactions*, A273, 463–485.
- Rabbitt, J.C. (1948) A new study of the anthophyllite series. *American Mineralogist*, 33, 263–323.
- Robertson, I.D.M., and Du Toit, M.C. (1981) Mobile belts. A. The Limpopo belt. In D.R. Hunter, Ed. *The Precambrian of the Southern Hemisphere*, 641–671. Elsevier, Amsterdam.
- Robinson, Peter, and Jaffe, H.W. (1969) Chemographic exploration of amphibole assemblages from central Massachusetts and southwestern New Hampshire. *Mineralogical Society of America Special Paper* 2, 251–274.
- Robinson, Peter, Ross, M., and Jaffe, H.W. (1971) Composition of the anthophyllite-gedrite series, comparisons of gedrite-hornblende, and the anthophyllite-gedrite solvus. *American Mineralogist*, 56, 1005–1041.
- Robinson, Peter, Spear, F.S., Schumacher, J.C., Laird, J., Klein, C., Evans, B.W., and Doolan, B.L. (1982) Phase relations in metamorphic amphiboles: Natural occurrence and theory. In D.R. Veblen and P.H. Ribbe, Eds. *Amphiboles: Petrology and experimental phase relations*, 1–227. Mineralogical Society of America Reviews in Mineralogy, 9b.
- Spear, F.S. (1978) Petrogenetic grid for amphibolites from the Post Pond Volcanics, Vermont. *Carnegie Institution of Washington Year Book* 77, 805–808.
- (1980) The gedrite-anthophyllite solvus and the composition limits of orthoamphibole from the Post Pond Volcanics, Vermont. *American Mineralogist*, 65, 1103–1118.
- (1982) Phase equilibria of amphibolites from the Post Pond Volcanics, Vermont. *Journal of Petrology*, 23, 383–426.
- Stout, J.H. (1970) Three-amphibole assemblages and their bearing on the anthophyllite-gedrite miscibility gap. (abs.). *American Mineralogist*, 55, 312–313.
- (1971) Four coexisting amphiboles from Telemark, Norway. *American Mineralogist*, 56, 212–224.
- (1972) Phase petrology and mineral chemistry of coexisting amphiboles from Telemark, Norway. *Journal of Petrology*, 13, 99–146.
- van Reenen, D.D. (1981) The southern marginal zone. In Barton, J.M., Jr, Ed. *Geology of the Limpopo belt. Limpopo Excursion Guidebook*, Geological Society of South Africa, 19–44.
- (1983a) Cordierite + garnet + hypersthene + biotite-bearing assemblages as a function of changing metamorphic conditions in the southern marginal zone of the Limpopo metamorphic complex, South Africa. *Geological Society of South Africa Special Publication* 8, 143–167.
- (1983b) Hydration of cordierite and hypersthene and the nature of the orthopyroxene isograd in the Limpopo belt, South Africa. *Geological Association of Canada/Mineralogical Association of Canada/Canadian Geophysical Union, Joint Annual Meeting, Victoria, Program with Abstracts*, 8, A72.
- van Reenen, D.D., and Du Toit, M.C. (1977) Mineral reactions and the timing of metamorphic events in the Limpopo metamorphic complex south of the Soutpansberg. *Geological Survey of Botswana Bulletin*, 12, 107–128.
- (1978) The reaction garnet + quartz = cordierite + hypersthene in granulites of the Limpopo metamorphic complex in northern Transvaal. *Geological Society of South Africa Special Publication* 4, 149–177.
- Vernon, R.H. (1972) Reactions involving hydration of cordierite and hypersthene. *Contributions to Mineralogy and Petrology*, 35, 125–137.

MANUSCRIPT RECEIVED APRIL 13, 1984

MANUSCRIPT ACCEPTED MARCH 18, 1986